ESI - Electronic Supplementary Information

$BaGe_8As_{14}$: a semiconducting sodalite type compound

Valentin Weippert, Thanh Chau, Kristian Witthaut, Lucien Eisenburger and Dirk Johrendt

EXPERIMENTAL

Synthesis. $BaGe_8As_{14}$ was synthesized via high temperature solid-state reactions. Stochiometric mixtures of Ba (99.99 % Sigma Aldrich), Ge (99.999 %, Sigma Aldrich) and As (99.99999+ %, Alfa Aesar) were filled in a corundum crucible and sealed in silica ampoules under an atmosphere of purified argon. To obtain suitable single crystals, the mixture was heated to 1123 K with a rate of 25 Kh^{-1}, kept at this temperature for 20 h and cooled to 673 K with a rate of 10 Kh^{-1} after which the furnace was switched off. For the synthesis of phase pure samples the mixture was heated to 873 K for 60 h with heating and cooling rates of 25 Kh^{-1}. After that the samples were thoroughly ground, pressed into pellets and treated with the same temperature program. This procedure was repeated twice. The reactions yielded either silver shards or black powder respectively. The compound is stable in air and water.

Single Crystal X-ray Diffraction. A suitable single crystal was isolated in paraffin oil and inserted and sealed into a glass capillary (Hilgenberg GmbH) of 0.2 mm in diameter. Single crystal data at room temperature was collected with a Bruker D8 Quest diffractometer ($Mo_{K\alpha}$, Photon-II detector). Low temperature single crystal data was collected between 293 and 105 K with a Bruker D8 Venture ($Mo_{K\alpha}$, Photon-II detector) equipped with a Kryoflex II cooling unit. Integration and absorption correction were performed with APEX3 and SADABS.[1, 2] The space group was determined with XPREP based on systematically absent reflections.[3] The phase problem was solved with Superflip and the model was refined with the SHELXL package.[4, 5]

The deposition numbers 2015241 (293 K), 2017129 (218 K), 2017128 (189 K), 2017127 (143 K) and 2017126 (103 K) contain the crystallographic data for this paper. These data are provided free of charge by the joint Cambridge Crystallographic Data Centre and Fachinformationszentrum Karlsruhe Access Structures service www.ccdc.cam.ac.uk/structures.

Powder X-ray Diffraction. A powdered sample was filled and sealed in a glass capillary (Hilgenberg GmbH) of 0.2 mm in diameter. The X-ray powder pattern was obtained with a Stoe Stadi-P diffractometer ($Cu_{K\alpha1}$, Ge(111)-monochromator, Mythen 1k detector). The Topas software package[6] was used for data analysis and Rietveld refinement of the model obtained from single crystal data.

High Temperature Powder X-ray Diffraction. A powdered sample was filled and sealed with grease in a silica capillary (Hilgenberg GmbH) of 0.4 mm in diameter. Data were collected between 298 and 1273 K with a Stoe Stadi P diffractometer ($Mo_{K\alpha1}$, Ge(111)-monochromator, IP-PSD detector) equipped with a graphite furnace. The data was analyzed with WinXPOW.[7]

EDX Measurements. A Carl Zeiss EVO-MA 10 with SE and BSE detectors controlled by the SmartSEM[8] software was used for scanning electron microscopy. EDX measurements were performed with the attached Bruker Nano EDX detector (X-Flash detector 410-M). Data evaluation was performed with the QUANTAX 200 software.[9] Signals from the aluminum sample holder and adhesive carbon tabs were disregarded.

UV-Vis-NIR Measurements. A diffuse reflectance spectrum of a powdered sample was measured with a VARIAN Cary 500 UV-Vis-NIR spectrophotometer equipped with a DRA-CA-5500 integrating sphere between 400 and 2000 nm. To account for the black color of $BaGe_8As_{14}$, the sample was mixed with $BaSO_4$. To determine optical bandgaps the data was converted based on the Kubelka-Munk theory.[10]

Resistivity and Hall Effect Measurements. A Sample was pressed into a pellet and sintered at 853 K for 60 h with heating and cooling rates of 50 Kh^{-1} in a corundum crucible sealed in a silica ampule under an atmosphere of purified argon. Resistivity and Hall Effect measurements were performed with a Quantum Design Inc. PPMS (physical property measurement system) equipped with a resistivity option.

The pellet was contacted with four point Van der Pauw press contact by Wimbush. Data were collected with the MultiVu software between 150 and 300 K with field strengths of ±50 kOe.[11]

TEM and STEM investigations. $BaGe_8As_{14}$ was ground in an agate mortar, suspended in pure ethanol and drop-cast on a TEM Grid with holey carbon film (Plano GmbH, Germany). The grid was mounted on a double-tilt holder and transferred into a Cs DCOR probe-corrected Titan Themis 300 (FEI, USA) TEM equipped with X-FEG, post-column filter (Enfinium ER-799), US1000XP/FT camera system (Gatan, Germany) and a windowless, 4-quadrant Super-X EDX detector. TEM images were recorded using a 4k × 4k FEI Ceta CMOS camera. The microscope was operated at 300 kV accelerating voltage for SAED and STEM-HAADF (convergence angle of 16.6 mrad, 50 µm aperture, detector inner half angle 33 mrad for 245 mm camera length). For evaluation of the TEM data, the following software was used: Digital Micrograph (Fourier filtering of STEM images), ProcessDiffraction7 (geometric calculations for SAED), JEMS (SAED simulations).[12-14]

DFT Calculations. We performed first principle electronic structure calculations with the Vienna Ab initio Simulation Package (VASP), [15, 16] based on density functional theory (DFT) and plane wave basis sets. Projector-augmented waves (PAW)[17] were applied and contributions of correlation and exchange were treated in the generalized-gradient approximation (GGA) using PBE,[18] PBEsol,[19] or SCAN[20] functionals. The Brillouin-zone was sampled with a 10×10×10 k-mesh. The structure parameters have been optimized until the energy changes are below 10^{-8} eV and forces between atoms below 10^{-3} eV/Å. To extract charges from the electron density we used the Bader analysis[21] implemented by Henkelman *et al*. [22] Mixed and fractional occupancies cannot be treated with VASP. Therefore, we reduced the symmetry of the structure to the subgroup $P\bar{4}3m$ (No. 215), which allows ordering of the mixed Ge/As site (8*c* to 2×4*e*). The split Ba position was idealized as fully occupied position (2*a*). The results of the structure relaxations are shown in Table S13 and Figure S8. The DOS and band structure were plotted using the sumo tools.[23]

Table S1. Detailed single crystal diffraction data of $BaGe_8As_{14}$

formula	$BaGe_8As_{14}$
space group	$I\bar{4}3m$ (No. 217)
a / Å	10.3145(2)
V_{cell} / Å^3	1097.35(6)
Z	2
$\rho_{X\text{-}ray}$ / g cm^{-3}	5.348
crystal size / mm	0.134 x 0.087 x 0.054
diffractometer	Bruker D8 QUEST
radiation type (λ / nm)	$Mo_{K\alpha}$ (0.71073)
T / K	293
μ / mm^{-1}	33.493
F(000)	1548
Θ-range / °	5.586 – 71.848
hkl range	-13 ≤ h ≤ 14; k ≤ ±14; -13 ≤ l ≤ +14
refl. measured	8373
independent refl.	329
parameters	16
R_σ / R_{int}	0.0113 / 0.0408
R_1 ($F^2 > 2\sigma(F^2)$) / all	0.0123 / 0.0132
wR_2 ($F^2 > 2\sigma(F^2)$) / all	0.0301 / 0.0303
GooF	1.330
$\Delta\rho_{max/min}$ / eÅ^{-3}	+0.597 / -0.598
constraints	5

Table S2. Atomic coordinates, equivalent displacement parameters (Å^2) and site occupancy factor (s.o.f.) of $BaGe_8As_{14}$ from single crystal data.

atom	Wyckoff	*x*	*y*	*z*	U_{eq}	s.o.f.
Ba1	8 *c*	0.47998(18)	0.47998(18)	0.47998(18)	0.0503(13)	0.25
Ge1	12 *d*	¼	½	0	0.01077(15)	1
Ge2	8 *c*	0.21902(5)	0.21902(5)	0.21902(5)	0.01339(18)	0.5
As1	24 *g*	0.38499(3)	0.38499(3)	0.15708(5)	0.01151(13)	1
As2	8 *c*	0.21902(5)	0.21902(5)	0.21902(5)	0.01339(18)	0.5

Table S3. Anisotropic displacement parameters (Å^2) of $BaGe_8As_{14}$ from single crystal data.

atom	U_{11}	U_{22}	U_{33}	U_{23}	U_{13}	U_{12}
Ba1	0.0503(13)	0.0503(13)	0.0503(13)	-0.0092(7)	-0.0092(7)	-0.0092(7)
Ge1	0.0129(3)	0.00973(18)	0.00973(18)	0	0	0
Ge2	0.01339(18)	0.01339(18)	0.01339(18)	0.00172(19)	0.00172(19)	0.00172(19)
As1	0.01216(16)	0.01216(16)	0.0102(2)	0.00053(12)	0.00053(12)	0.00034(16)
As2	0.01339(18)	0.01339(18)	0.01339(18)	0.00172(19)	0.00172(19)	0.00172(19)

Table S4. Selected distances (Å) of $BaGe_8As_{14}$.

atoms	distance	atoms	distance
Ba1 — As1	3.6073(19)	Ba1 — As1	4.1126(19)
Ba1 — As1	3.6073(19)	Ba1 — As1	4.1126(19)
Ba1 — As1	3.6073(19)	Ba1 — Ge2|As2	4.2705(19)
Ba1 — Ge2|As2	3.8086(19)	Ge1 — As1	2.4436(4)
Ba1 — Ge2|As2	3.8086(19)	Ge1 — As1	2.4436(4)
Ba1 — Ge2|As2	3.8086(19)	Ge1 — As1	2.4436(4)
Ba1 — As1	3.8694(19)	Ge1 — As1	2.4436(4)
Ba1 — As1	3.8694(19)	Ge2|As2 — As1	2.5039(7)
Ba1 — As1	3.8694(19)	Ge2|As2 — As1	2.5039(7)
Ba1 — As1	4.1126(19)	Ge2|As2 — As1	2.5039(6)
Ba1 — As1	4.1126(19)	As1 — Ge1	2.4436(4)
Ba1 — As1	4.1126(19)	As1 — Ge1	2.4436(4)
Ba1 — As1	4.1126(19)	As1 — Ge2|As2	2.5039(6)

Table S5. Detailed single crystal diffraction data of $BaGe_8As_{14}$ at 218, 189, 143 and 103 K

formula	$BaGe_8As_{14}$			
space group	$I\bar{4}3m$ (No. 217)			
a / Å	10.3060(2)	10.3052(2)	10.3018(2)	10.2967(2)
V_{cell} / Å^3	1094.64(6)	1094.38(6)	1093.30(6)	1091.68(6)
Z	2			
$\rho_{X\text{-}ray}$ / g cm^{-3}	5.361	5.362	5.367	5.375
crystal size / mm	0.059 x 0.111 x 0.119			
diffractometer	Bruker D8 VENTURE			
radiation type (λ / nm)	$Mo_{K\alpha}$ (0.71073)			
T / K	218	189	143	103
μ / mm^{-1}	33.576	33.584	33.617	33.667
F(000)	1548			
Θ-range / °	5.590 – 89.110	5.591 – 89.118	5.592 – 90.793	5.595 – 89.211
hkl range	± 17			
refl. measured	17101	17257	17366	17494
independent refl.	540	541	542	547
parameters	16			
R_σ / R_{int}	0.0098 / 0.0355	0.0100 / 0.0373	0.0100 / 0.0358	0.0105 / 0.0395
R_1 ($F^2 > 2\sigma(F^2)$) / all	0.0116 / 0.0120	0.0119 / 0.0119	0.0117 / 0.0119	0.0119 / 0.0121
wR_2 ($F^2 > 2\sigma(F^2)$) / all	0.0373 / 0.0374	0.0366 / 0.0366	0.0364 / 0.0364	0.0345 / 0.0346
GooF	1.418	1.431	1.468	1.351
$\Delta\rho_{max/min}$ / eÅ^{-3}	+0.870 / -0.436	+1.105 / -0.741	+0.840 / -0.688	+1.266 / -0.524
constraints	5			

Table S6. Atomic coordinates*, equivalent displacement parameters (Å^2) and site occupancy factor (s.o.f.) of $BaGe_8As_{14}$ from single crystal data at 218 K.

atom	Wyckoff	x	y	z	U_{eq}	s.o.f.
Ba1	8 c	0.01986(18)	0.01986(18)	0.01986(18)	0.0446(12)	0.25
Ge1	12 d	¼	½	0	0.00792(11)	1
Ge2	8 c	0.28102(5)	0.28102(5)	0.28102(5)	0.01021(15)	0.5
As1	24 g	0.11512(4)	0.11512(4)	0.34292(5)	0.00855(9)	1
As2	8 c	0.28102(5)	0.28102(5)	0.28102(5)	0.01021(15)	0.5

*Inverted structure compared to Table S4 due to Flack parameter requirements.

Table S7 Anisotropic displacement parameters (Å^2) of $BaGe_8As_{14}$ from single crystal data at 218 K.

atom	U_{11}	U_{22}	U_{33}	U_{23}	U_{13}	U_{12}
Ba1	0.0446(12)	0.0446(12)	0.0446(12)	-0.0092(6)	-0.0092(6)	-0.0092(6)
Ge1	0.0098(3)	0.00699(15)	0.00699(15)	0	0	0
Ge2	0.01021(15)	0.01021(15)	0.01021(15)	0.00186(17)	0.00186(17)	0.00186(17)
As1	0.00894(12)	0.00894(12)	0.00776(18)	0.00054(10)	0.00054(10)	0.00035(14)
As2	0.01021(15)	0.01021(15)	0.01021(15)	0.00186(17)	0.00186(17)	0.00186(17)

Table S8. Atomic coordinates, equivalent displacement parameters (Å^2) and site occupancy factor (s.o.f.) of $BaGe_8As_{14}$ from single crystal data at 189 K.

atom	Wyckoff	*x*	*y*	*z*	U_{eq}	s.o.f.
Ba1	8 c	0.01981(17)	0.01981(17)	0.01981(17)	0.0417(12)	0.25
Ge1	12 d	¼	½	0	0.00687(11)	1
Ge2	8 c	0.28105(5)	0.28105(5)	0.28105(5)	0.00895(15)	0.5
As1	24 g	0.11513(4)	0.11513(4)	0.34287(5)	0.00742(9)	1
As2	8 c	0.28105(5)	0.28105(5)	0.28105(5)	0.00895(15)	0.5

Table S9. Anisotropic displacement parameters (Å^2) of $BaGe_8As_{14}$ from single crystal data at 189 K.

atom	U_{11}	U_{22}	U_{33}	U_{23}	U_{13}	U_{12}
Ba1	0.0417(12)	0.0417(12)	0.0417(12)	-0.0091(6)	-0.0091(6)	-0.0091(6)
Ge1	0.0085(2)	0.00603(15)	0.00603(15)	0	0	0
Ge2	0.00895(15)	0.00895(15)	0.00895(15)	0.00170(16)	0.00170(16)	0.00170(16)
As1	0.00781(12)	0.00781(12)	0.00662(18)	0.00045(10)	0.00045(10)	0.00030(13)
As2	0.00895(15)	0.00895(15)	0.00895(15)	0.00170(16)	0.00170(16)	0.00170(16)

Table S10. Atomic coordinates, equivalent displacement parameters (Å^2) and site occupancy factor (s.o.f.) of $BaGe_8As_{14}$ from single crystal data at 143 K.

atom	Wyckoff	*x*	*y*	*z*	U_{eq}	s.o.f.
Ba1	8 c	0.01979(16)	0.01979(16)	0.01979(16)	0.0388(11)	0.25
Ge1	12 d	¼	½	0	0.00598(11)	1
Ge2	8 c	0.28107(5)	0.28107(5)	0.28107(5)	0.00799(14)	0.5
As1	24 g	0.11513(3)	0.11513(3)	0.34287(5)	0.00649(9)	1
As2	8 c	0.28107(5)	0.28107(5)	0.28107(5)	0.00799(14)	0.5

Table S11. Anisotropic displacement parameters (Å^2) of $BaGe_8As_{14}$ from single crystal data at 143 K.

atom	U_{11}	U_{22}	U_{33}	U_{23}	U_{13}	U_{12}
Ba1	0.0388(11)	0.0388(11)	0.0388(11)	-0.0092(5)	-0.0092(5)	-0.0092(5)
Ge1	0.0075(2)	0.00524(15)	0.00524(15)	0	0	0
Ge2	0.00799(14)	0.00799(14)	0.00799(14)	0.00174(16)	0.00174(16)	0.00174(16)
As1	0.00677(12)	0.00677(12)	0.00593(17)	0.00044(10)	0.00044(10)	0.00032(13)
As2	0.00799(14)	0.00799(14)	0.00799(14)	0.00174(16)	0.00174(16)	0.00174(16)

Table S12. Atomic coordinates, equivalent displacement parameters (Å^2) and site occupancy factor (s.o.f.) of $BaGe_8As_{14}$ from single crystal data at 103 K.

atom	Wyckoff	*x*	*y*	*z*	U_{eq}	s.o.f.
Ba1	8 c	0.01987(15)	0.01987(15)	0.01987(15)	0.0340(10)	0.25
Ge1	12 d	¼	½	0	0.00409(10)	1
Ge2	8 c	0.28112(5)	0.28112(5)	0.28112(5)	0.00593(14)	0.5
As1	24 g	0.11514(3)	0.11514(3)	0.34284(5)	0.00459(8)	1
As2	8 c	0.28112(5)	0.28112(5)	0.28112(5)	0.00593(14)	0.5

Table S13. Anisotropic displacement parameters (Å^2) of $BaGe_8As_{14}$ from single crystal data at 103 K.

atom	U_{11}	U_{22}	U_{33}	U_{23}	U_{13}	U_{12}
Ba1	0.0340(10)	0.0340(10)	0.0340(10)	-0.0089(5)	-0.0089(5)	-0.0089(5)
Ge1	0.0054(2)	0.00345(14)	0.00345(14)	0	0	0
Ge2	0.00593(14)	0.00593(14)	0.00593(14)	0.00172(15)	0.00172(15)	0.00172(15)
As1	0.00481(11)	0.00481(11)	0.00413(17)	0.00043(10)	0.00043(10)	0.00028(13)
As2	0.00593(14)	0.00593(14)	0.00593(14)	0.00172(15)	0.00172(15)	0.00172(15)

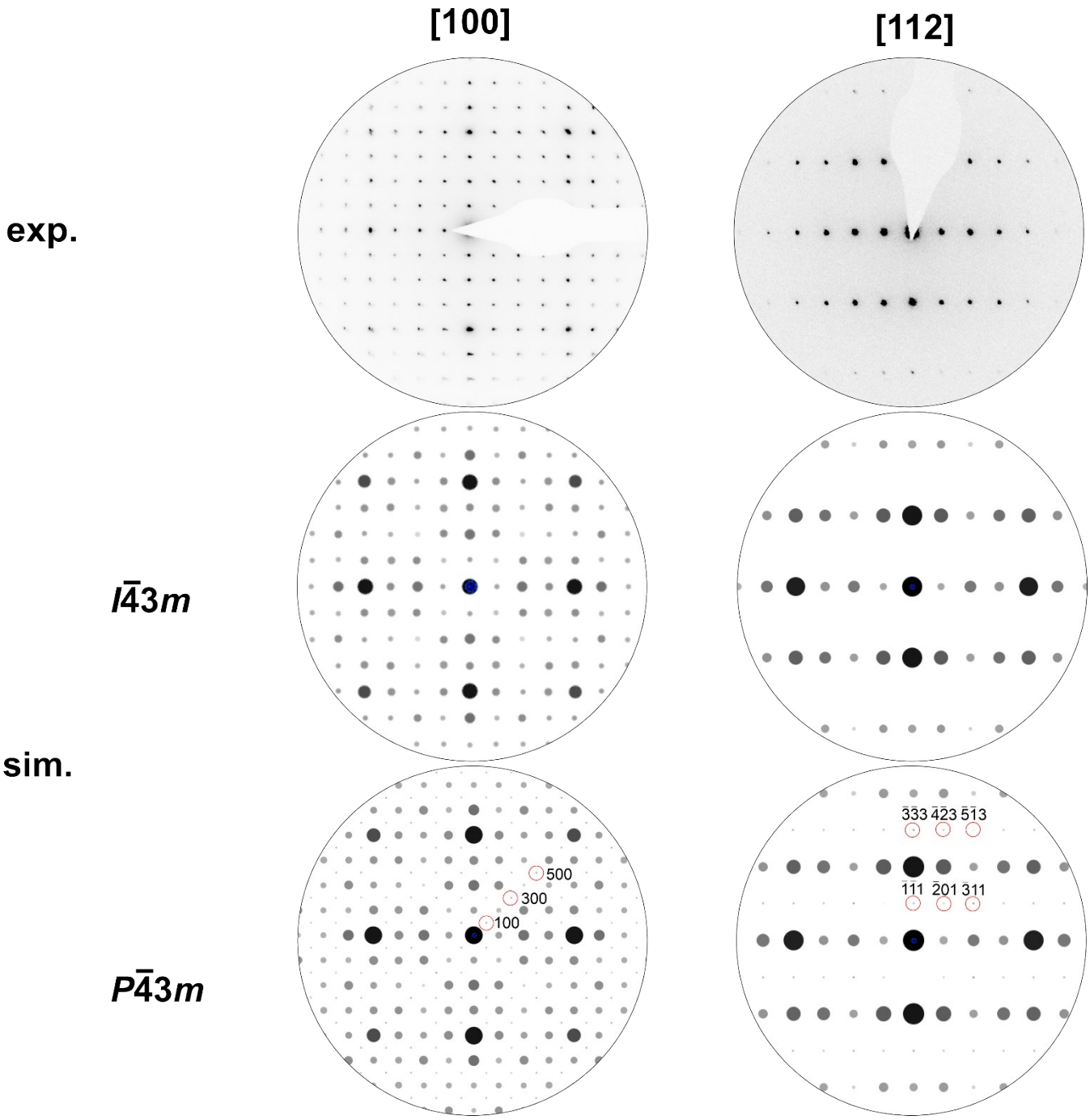

Figure S1. *Top*: SAED pattern of $BaGe_8As_{14}$ in [100] and [112] direction on thick crystals to enhance the effects of dynamical diffraction (enable violation of systematical absences due to multiple scattering). *Middle*: Simulated SAED patterns of $BaGe_8As_{14}$ with the space group $I\bar{4}3m$ (No. 217) as obtained from single crystal X-ray diffraction with a mixed occupied Ge/As position (8c). *Bottom*: Simulated SAED pattern of $BaGe_8As_{14}$ in the *klassengleiche* subgroup $P\bar{4}3m$ (No. 215) with ordered Ge (4e) and As (4e) positions. Selected additional reflexes are highlighted (red) and indexed. These do not appear in the experimental pattern.

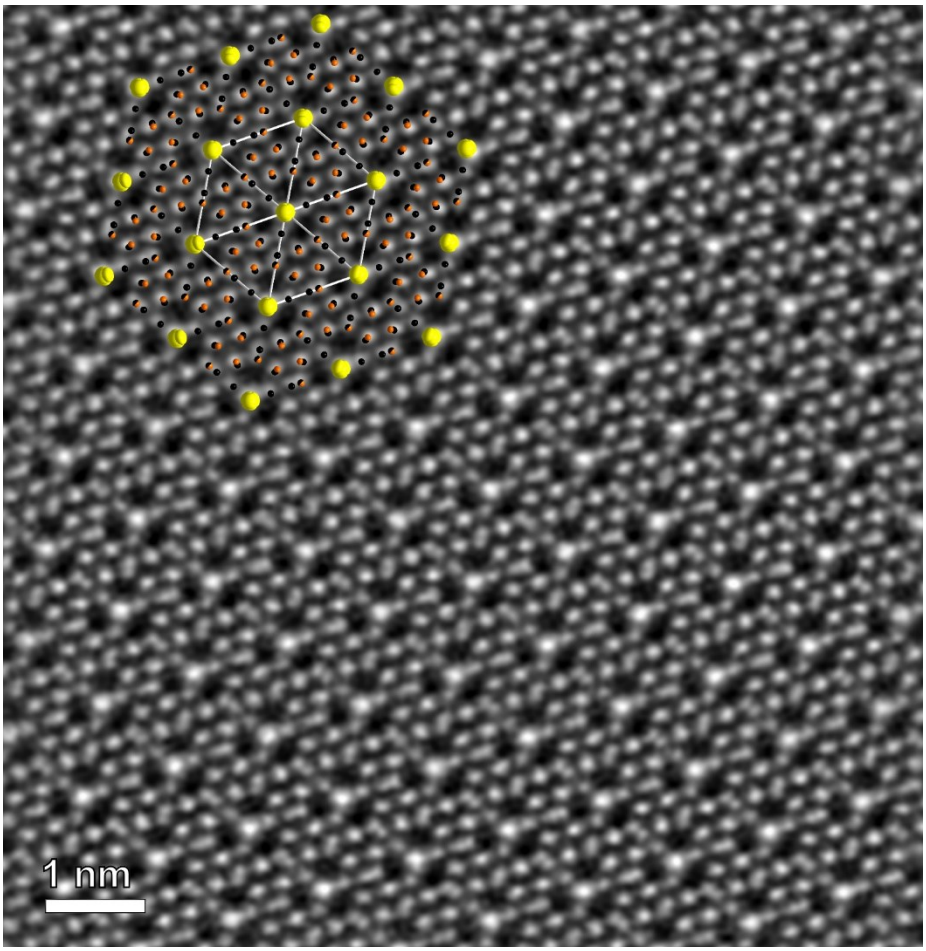

Figure S2. STEM HAADF image of $BaGe_8As_{14}$ in [111] direction with overlay (Ba: yellow, Ge: brown, As: black).

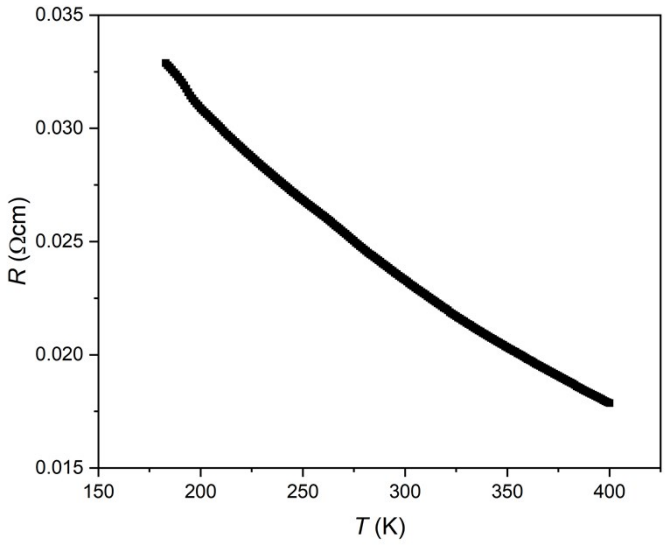

Figure S3. Resistivity of $BaGe_8As_{14}$ between 400 K and 180 K.

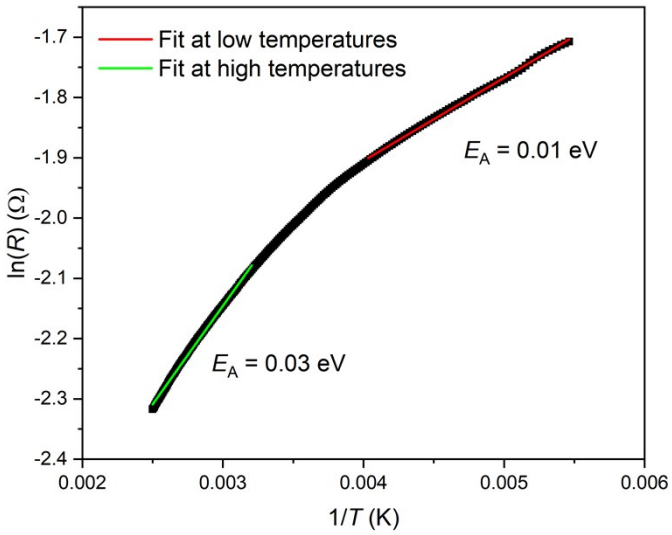

Figure S4. Arrhenius plot of the resistivity of $BaGe_8As_{14}$ showing a band gap of 0.03 eV at high temperatures and a band gap of 0.01 eV at low temperatures.

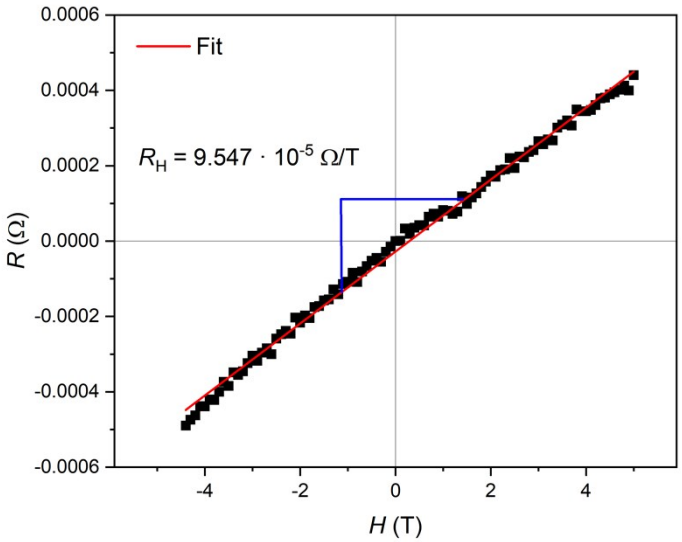

Figure S5. Hall Effect measurement of $BaGe_8As_{14}$ at 300 K yielding a positive Hall resistance of 9.547 · 10^{-5} Ω/T. This results in a carrier concentration of $1.6 \cdot 10^{20}$ cm^{-3} and a mobility μ of 1.6 $cm^2V^{-1}s^{-1}$.

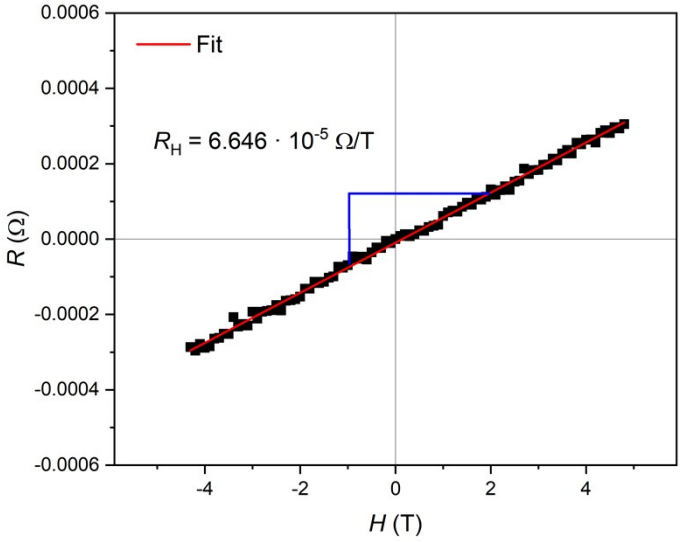

Figure S6. Hall Effect measurement of $BaGe_8As_{14}$ at 400 K yielding a positive Hall resistance of 6.646 · 10^{-5} Ω/T. This results in a carrier concentration of $2.3 \cdot 10^{20}$ cm^{-3} and a mobility μ of 1.5 $cm^2V^{-1}s^{-1}$.

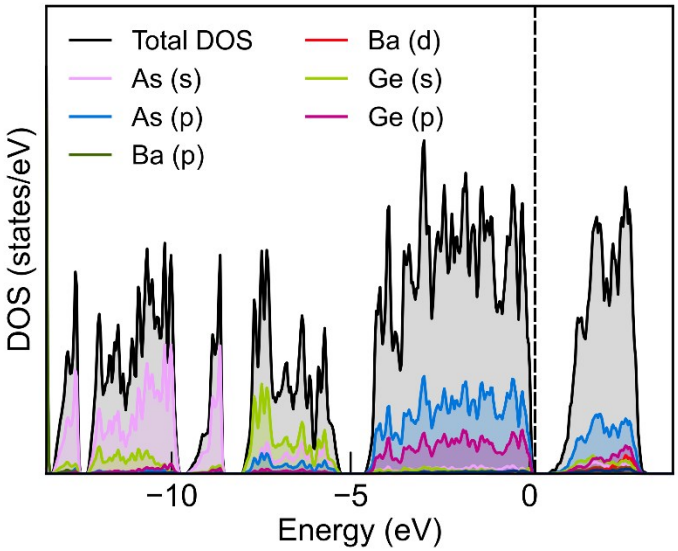

Figure S7. Total and atom projected density of states (DOS) of $BaGe_8As_{14}$ calculated with PBE functional. The energy zero is taken at the Fermi level Fermi (dashed line).

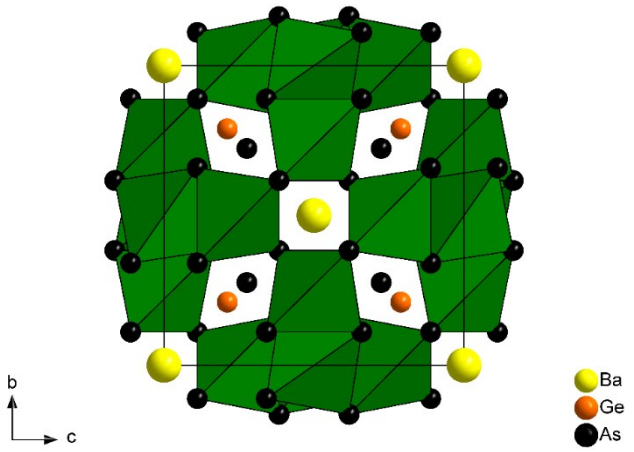

Figure S8. Unit cell of $BaGe_8As_{14}$ in the subgroup $P\bar{4}3m$ with ordered Ge and As positions.

Table S14. Calculated parameters for $BaGe_8As_{14}$ (VASP, PBE)

Lattice parameter a = 10.487 Å, space group $P\bar{4}3m$

Atom	Wyckoff	x	y	z
Ba1	1*a*	0	0	0
Ba2	1*b*	½	½	½
Ge1	12*h*	0.2543	½	½
Ge2	4e	0.7177	x	x
As1	4*e*	0.2252	x	x
As2	12*i*	0.3873	x	0.1554
As3	12*i*	0.8813	x	0.6601

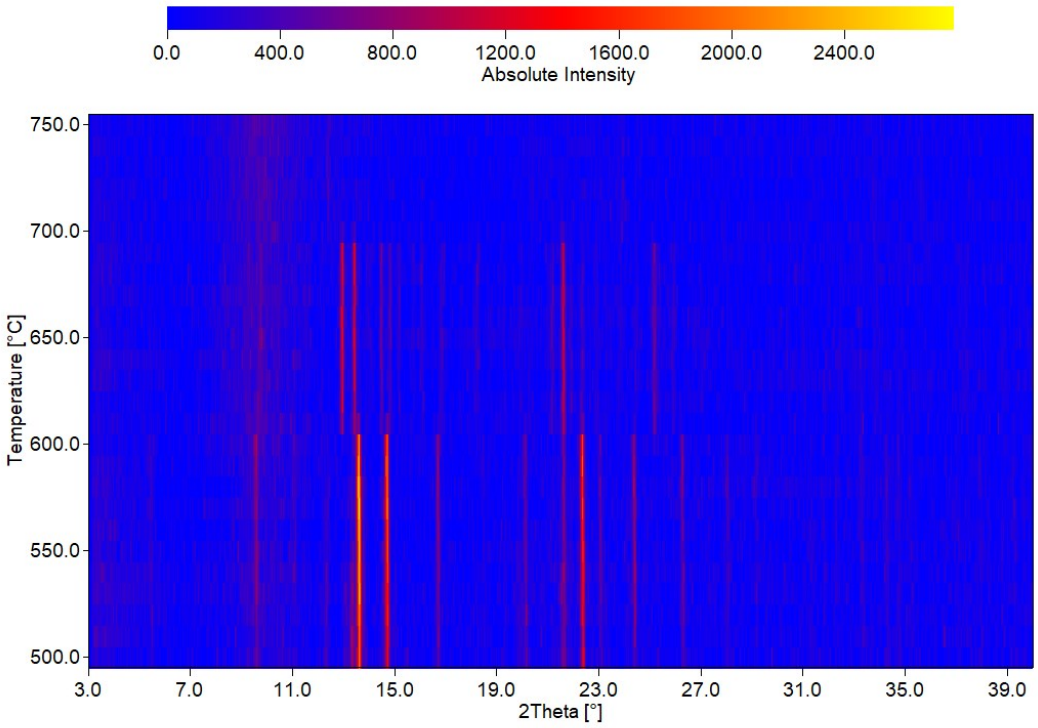

Figure S9. High temperature powder X-ray diffraction patterns ($Mo_{K\alpha1}$) of $BaGe_8As_{14}$ between 773 K and 1023 K with steps of 10 K: Intensities of $BaGe_8As_{14}$ are decreasing for T > 873 K.

Table S15. Powder X-ray diffraction data of $BaGe_8As_{14}$ from Rietveld refinement.

formula	$BaGe_8As_{14}$
space group	$I\bar{4}3m$ (No. 217)
a / Å	10.312605(63)
V_{cell} / Å^3	1096.744(20)
Z	2
$\rho_{X\text{-}ray}$ / g cm^{-3}	5.3518(2)
diffractometer	Stoe Stadi P
radiation type (λ / nm)	$Cu_{K\alpha1}$ (1.54056)
T / K	293
μ / mm^{-1}	49.0492(9)
2Θ-range / °	5.000 - 92.420
parameters (incl. side phases	30
background parameter	12
R_p / R_{wp}	4.524 / 6.788
R_{exp} / R_{Bragg}	2.570 / 2.139
GooF	2.641

References

1. APEX3, v2016.5-0 ed., Bruker AXS Inc., Madison, USA, 2016.
2. SADABS, Version 2012/1 ed., Bruker AXS Inc., Madison,USA, 2001.
3. XPREP, Version 2008/2 ed., Bruker AXS Inc., Madison, USA, 2008.
4. L. Palatinus and G. Chapuis, *J. Appl. Crystallogr.*, 2007, **40**, 786-790.
5. G. Sheldrick, *Acta Crystallogr., Sect. C: Struct. Chem.*, 2015, **71**, 3-8.
6. TOPAS Academics, 6 ed., Coelho Software, Brisbane, Australia, 2016.
7. WinXPOW, Version 3.0.2.5 ed., STOE & Cie GmbH, Darmstadt, Germany, 2011.
8. SmartSEM, Version 5.07 Beta ed., Carl Zeiss Microscopy Ltd., Cambridge, UK, 2014.
9. QUANTAX 200, Version 1.9.4.3448 ed., Bruker Nano GmbH, Berlin, Germany, 2013.
10. P. Kubelka and F. Munk, *Z. Tech. Phys.*, 1931, **12**, 593-601.
11. MultiVu, Version 1.5.11 ed., Quantum Design Inc., San Diego, USA, 2013.
12. DigitalMicrograph, 3.6.1 ed., Gatan Software Team, 1999.
13. ProcessDiffraction7, 7.3.2 Q ed., 2012.
14. JEMS, 3.3425 ed., 2008.
15. G. Kresse and J. Hafner, *Phys. Rev. B*, 1994, **49**, 14251-14269.
16. G. Kresse and J. Furthmüller, *Comput. Mater. Sci.*, 1996, **6**, 15-50.
17. P. E. Blöchl, *Phys. Rev. B*, 1994, **50**, 17953-17979.
18. J. P. Perdew, K. Burke and M. Ernzerhof, *Phys. Rev. Lett.*, 1996, **77**, 3865-3868.
19. J. P. Perdew, A. Ruzsinszky, G. I. Csonka, O. A. Vydrov, G. E. Scuseria, L. A. Constantin, X. Zhou and K. Burke, *Phys. Rev. Lett.*, 2008, **100**, 136406.
20. J. Sun, A. Ruzsinszky and J. P. Perdew, *Phys. Rev. Lett.*, 2015, **115**, 036402.
21. R. F. W. Bader, *Atoms in Molecules - A Quantum Theory*, Oxford University Press, London, 1990.
22. G. Henkelman, A. Arnaldsson and H. Jónsson, *Comput. Mater. Sci.*, 2006, **36**, 354-360.
23. A. M. Ganose;, A. J. Jackson; and D. O. Scanlon;, *Journal of Open Source Software*, 2018, **3**, 717.